

The Electromagnetic Considerations of the Nuclear Force

N. L. Bowen¹

¹Colorado Mountain College, Glenwood Springs, Colorado, USA

*corresponding author, E-mail: nbowen@coloradomtn.edu

Abstract

This paper explores how the electromagnetic energies of the quarks within the nucleus affect the behavior of the Nuclear Force. By examining the electromagnetic energies and forces, many questions about nuclear behavior can be answered and many insights into the nucleus can be gained. Previous theoretical models for the nuclear force include only the Coulomb electric force of the protons, but with little or no consideration of the electromagnetic characteristics of the quarks. By incorporating the electromagnetic energies and forces into nuclear theory, this model has been able to achieve predictions of binding energy better than any previous model, doing so by using only one variable instead of five. This model unifies the nuclear force to the electromagnetic force.

1. Introduction

1.1. Definition and Clarification of terms

The “Nuclear Force” is that force which binds together the nucleons in the nucleus. Historically, the Nuclear Force was called the “Strong Nuclear Force”, and was considered to be one of the four forces of nature, along with the gravitational force, the electromagnetic force and the weak nuclear force. Soon after the discovery of quarks, the force which holds the quarks together in a nucleon was called the “Chromo Dynamic Force”. This Chromo Dynamic Force, which is a sub-nucleon force, is considered to be much larger than the Nuclear Force. Later, the Chromo Dynamic Force was redefined as the Strong Nuclear Force, which is now considered to be a sub-nucleon force responsible for the behavior and interactions of sub-nucleon particles. The force which hold the nucleons together in a nucleus was renamed as the “Nuclear Force”. To add to the confusion even more, there is a model of the Nuclear Force, which is called the Residual Chromo Dynamic Force. This model is a model of the Nuclear Force, that force which holds the nucleons together inside a nucleus. Because of this model, it is presumed that the Nuclear Force is simply a subset of the Strong Nuclear Force. Because of this association, it is still claimed that there are only four forces in Nature: The Strong Nuclear Force, the Electromagnetic Force, the Gravitational Force, and the Weak Nuclear Force. The Strong Nuclear Force has two parts, the Chromo Dynamic force which is sub-nucleon, and the Nuclear Force, which is that force holding the nucleons together in a nucleus.

For clarity to the reader in this paper, the term Strong Nuclear Force will not be used. Rather the term Chromo Dynamic Force will be used to reference that force which holds together the quarks inside a nucleon. The term Nuclear Force will be used to describe that force which holds together the nucleons in a nucleus. The term Residual Chromo Dynamic Force will be used to describe one of the models of the Nuclear Force, and it will be emphasized in italics as the *Residual* Chromo Dynamic Force, to avoid any confusion of this force with the Chromo Dynamic Force.

1.2. Electromagnetics and the Nuclear Force

The development of a proper theory of the nuclear force has occupied nuclear physicists for over eight decades and has been one of the main topics of physics research in the 20th and 21st centuries. The focus of this paper is the role of electromagnetic energies within the nucleus and how these energies affect nuclear behavior. The emphasis of this paper is electromagnetics, since this has been largely disregarded in previous models of the nuclear force. Although the emphasis is on electromagnetics, this paper does not ignore quantum physics in any way, and the concepts of quantum physics are included in this paper.

Currently, there is no one model of the nuclear force that can explain the majority of nuclear behaviors [1, 2, 3, 4]. Here is a brief list of the more salient nuclear behaviors that a successful model of the nuclear force should address:

- Particle decay—this includes alpha decay, beta-delayed alpha decay, proton decay, beta-delayed proton decay, neutron decay, beta-delayed neutron decay, spontaneous fission, and beta-delayed spontaneous fission. (Beta decay and gamma decay are not considered as particle decay.)
- The shape of binding energy curve.
- Large quadrupole moments.
- Why and how excited energy states exist.

In this paper, the lowest energy configuration of hundreds of nuclides, from ²H to ²⁰⁸Pb, have been computer-modeled and simulated, by applying the laws of electromagnetics to the quarks inside of the nucleus. The binding energies of these nuclides have been calculated and compared to experimental data. Using only electromagnetics to compute the binding energies, the calculated binding energies agree with the experimental binding energies within a few percent. These computations are done

by using only one variable, rather than five variables. (The Weizsäcker formula, which is a curve-fitting equation, uses five variables plus conditional logic to empirically curve-fit the experimental data.) No other current theoretical model of the nuclear force has been able to demonstrate such a tight prediction of binding energy for all the nuclides from ${}^2\text{H}$ to ${}^{208}\text{Pb}$ with only one variable. This achievement is an unprecedented success and strongly indicates the correctness of this new model.

1.3. Current Concepts Regarding the Chromo Dynamic Force

The Chromo Dynamic Force is thought to be much stronger than the Nuclear Force, by several orders of magnitude. However, an actual definitive measurement of the strength of this force has not been made because particle physicists have been unable to separate the quarks inside a nucleon. Presently there are numerous models, some of which are quite complex and confusing, about what is inside a nucleon. These models attempt to describe the number of quarks inside a nucleon, what components make up the bulk mass of a nucleon, and what gives a nucleon its spin. Particle physicists believe that there could be several hundred non-valence quarks inside a nucleon. Suffice it to say, particle physicists are not presently concerned about applying uncertainty principles to these hundreds of quarks. The motion of the non-valence quarks is presumed to contribute to the orbital angular momentum of the nucleon, along with the massless gluons that hold them together; however, this has not been confirmed experimentally. It is not the intention of this paper to be a critique or review of the models of the sub-nucleon Chromo Dynamic Force. In this paper, only the three valence quarks are considered.

2. Brief Review of Current Models

There are numerous models for the nuclear force. Each model can provide some explanation of certain properties of nuclei in their ground state, but no single model can explain all the properties. No complete theory exists which fully describes the structure and behavior of the nuclear force and of the nuclei which it controls [1, 2, 3, 4]. Listed below are brief descriptions of the more-commonly known nuclear models.

2.1. Gamow's Alpha Decay Model

One of the first descriptions for nuclear behavior was developed in 1928 by G. Gamow [5] to explain the observed alpha decay for the large nuclides. This proposed mechanism uses the Schrödinger equation to describe how an alpha particle can overcome its potential barrier via quantum tunneling. Gamow's proposed mechanism is valid only for the larger nuclides and does not apply to the near-instantaneous alpha decay seen in several of the smaller nuclides. Although the tunneling mechanism serves as a good description for the process of large-A alpha decay, it assumes the alpha particle is pre-formed inside the nucleus, an idea contrary to the independent particle models.

2.2. Weizsäcker Formula and the Liquid Drop Model

The Weizsäcker formula [6] is simply a mathematical equation used to curve-fit the experimental binding energy data. This formula is also known as the semi-empirical mass formula, meaning that the variables are chosen to curve-fit the data empirically. It uses five variables and conditional logic to obtain the best fit to the experimental binding curve. Although this curve-fitting formula is not a model *per se*, it is used in conjunction with the liquid drop model.

The liquid drop model, developed by Gamow in 1929 [7], states that nucleons bind only to their closest neighbors, as in a drop of liquid. This concept is based on the experimental binding energy curve, for which the energy per nucleon is relatively constant; this behavior is caused by the limited number of times that a nucleon can bind with other nucleons. (Interestingly, this limitation is also true of the atomic bond within crystals. An atom in a crystal can bond only to its nearest neighbors, thus the number of bonds which can be formed by a single atom is limited.) The liquid drop model assumes the nucleus is spherical. In conjunction with the curve-fitting Weizsäcker formula, the liquid drop model can predict the experimental binding energies to within a few percent. The liquid drop model offers only a conceptual explanation for spontaneous fission, but it does not offer a rigorous mathematical description for this behavior. For example, it can not explain why certain nuclides such as ${}^{237}\text{Cf}$ exhibit fission, but other larger ones, such as ${}^{275}\text{Hs}$ do not. The liquid drop model does not consider excited states, large quadrupole moments, or other types of nuclear particle decay.

2.3. Meson Exchange Model

In 1935, Hideki Yukawa proposed that the nuclear interaction was mediated by an exchange of mesons [8]. This meson exchange model served, for many years, as a good description for the underlying mechanism of nuclear binding. However, the model itself does not attempt to explain binding energies, particle decay, excited states, or large quadrupole moments.

2.4. Alpha Cluster Model

The alpha-cluster model was developed in 1938 [9] to explain the stronger binding energy that is experimentally observed for nuclei with an integer number of alpha particles. When used in conjunction with the alpha decay model [5], together these

models can explain the mechanism for alpha decay of the large isotopes, as well as correlating the experimentally-observed energy of the emitted alpha particles to the half-life of the alpha decay. Recently, there has been much experimental evidence that excited states of nuclides are indeed made of clusters of alpha particles [10,11,12,13,14,15], as well as other building blocks. More recent theoretical refinements of the alpha-cluster model have provided increasing insight into these experimental observations [16,17,18,19,20,21, 22, 23].

2.5. Independent Particle Model

There are several independent particle models of the nuclear force, of which the Fermi gas model [24] is the simplest. These models hypothesize that nucleons move independently, confined inside a three-dimensional energy well, and that the nucleons do not interact with each other to any significant extent. By using this concept, these independent particle models are much easier to solve mathematically than an n-body problem of the nucleus. The more complex independent-particle models alter the shape of the potential energy well, from that of the Fermi gas model, by using numerous variables depending on the nuclide being studied. This alteration is done to predict the excited states of the nuclide. However, these independent-particle models can not explain large quadrupole moments, unless a non-radial energy well is pre-assumed for the Hamiltonian. These models do not attempt to explain the binding energy curve or particle decay.

2.6. Shell Model

The nuclear shell model was first hypothesized in 1932 and further developed in 1949 [25, 26, 27]. It is considered to be an independent-particle model, based on a concept similar to the electronic shell structure of atoms. The model is an attempt to explain the minor deviations that have been observed between experimental data and the Weizsäcker formula. This model assumes there is a passive nuclear core of nucleons, beyond which only the valence nucleons contribute to the nuclear behavior. The shells are based on “magic” numbers. When experimental data is compared to the Weizsäcker formula, the inconsistencies are observed to be larger at these magic numbers. Another experimental observation of magic numbers, unrelated to the Weizsäcker formula, is that for the lowest excited spin-2 state of the even-even nuclides, the energy is a higher for the nuclides with magic numbers than for nuclides with non-magic numbers. Another experimental observation of magic numbers is that the neutron separation energy has a slight step for the nuclides when N is equal to a magic number.

Theoretically, to get these magic numbers, the shell model starts from a potential well called the “Woods-Saxon” potential. This potential energy well lies somewhere between the abrupt square well and the smooth harmonic-oscillator well; it also asymptotically approaches a zero energy at the well boundary. To this Woods-Saxon potential, a spin-orbit term is added, in an attempt to duplicate the observed magic numbers. However, the result does not coincide with these magic numbers unless an empirical spin-orbit coupling is also added. The shell model does not explain any type of particle decay or large quadrupole moments [28]. The shell model uses the Pauli Exclusion Principle to predict spins; however, it can only do this accurately if the Nilsson terms are included [28]. The Nilsson term is not a “term” in the strict mathematical sense of the word; rather it is at least two or three different variables, with values that are dependent on the nucleus being studied. These are often referred to as “spaghetti plots” due to their complicated natures. When the Nilsson terms are included into the spin-orbit coupling constant, a better prediction of the nuclear spins can be achieved [29].

2.7. Collective Model

Another model is the Bohr-Mottelson model, also known as the collective model [30, 31, 32, 33, 34]. This model is described as a combination the essential features of the liquid drop model and the shell model. In the shell model, one regards the primary form of motion as the orbital motion of the individual nucleons in the average nuclear field. However, in the liquid-drop model one looks at the simple collective motions of the nucleons. Both of these forms of motions are observed experimentally in nuclei to some extent. Thus, the Bohr-Mottelson model is a more general description of nuclear structure, one that considers the total state of motion as a superposition of these two basic components of motion. Such a description is regarded as a generalization of the shell model, in which the nuclear field is no longer considered to be considered constant, but rather to be considered to be a dynamic variable, in that the net nuclear potential undergoes deformations away from a spherical well. The Schrödinger equation is solved for non-spherical net nuclear potential. This variation of the collective nuclear field is linked with the vibrating shape of the nucleus. By using this dynamically-variable nuclear field the Bohr-Mottelson model can more closely estimate magnetic dipole moments and large electric quadrupole moments.

2.8. Collective-Motion Model

The collective-motion model (not to be confused with the collective model) is more of an experimental observation than a model. The experimentally-measured spin energies of the nucleus indicate that the nucleus is not a collection of independent particles moving randomly with respect to each other, but rather the rotational moment of inertia of the nucleus is similar to a rigid structure. This behavior is referred to as an apparent collective motion of the nucleus [35, 36] whereby the nucleons within the nucleus appear to move with a collective motion.

2.9. Effective Field Model

Several other models are grouped together under the term “effective field models” [37]. These models incorporate an approximation for the overall Hamiltonian, often times using as many as 40 or more variables to curve fit the predicted results to the observed experimental data [38]. These effective field models are used to explain results from scattering experiments.

2.10. Residual Chromo dynamic Model

The residual chromo dynamic model [39], similar to the meson exchange model of 1935, postulates that the nuclear force is caused by the exchange of virtual light mesons, such as the virtual pi-mesons (aka pions). In this model, the nuclear force is produced by a potential energy well that is a residual short-range force of the chromo dynamic force. The chromo dynamic force is the force that holds the quarks together *inside* the nucleon, in which dissimilar colors are attracted to each other, but similar colors are not. Conversely, the *residual* chromo dynamic force occurs *outside* the nucleon. It is postulated that this residual force bonds the quarks in one nucleon to a quark in another nucleon. The *residual* chromo dynamic force thereby binds the two nucleons together. In other words, the residual chromo dynamic force is an inter-nucleon force between two quarks. The residual chromo dynamic force is often compared to the Van der Waals force, a force that is electromagnetic in nature, due to the electric dipole moment of the molecules. Fig. 1 depicts the residual chromo dynamic force for a deuterium nucleus, showing the quarks, (red, blue and green). The chromo dynamic forces are represented in Fig. 1 by the bond black lines, and the residual chromo dynamic force is represented by the gray dotted line.

The proton is composed of one down quark and two up quarks; the neutron is composed of one up quark and two down quarks. The quarks are shown in the colors of red, green, and blue. The chromo dynamic force is represented by the darker coils in the nucleons. The lighter coils represent the *residual* chromo dynamic force, between the nucleons.

With regard to quantum chromo dynamics, the word “color” has no relation to visible color. Also, the terms “up” and “down” have no relationship to vertical direction. Similar to the liquid drop model, the *residual* chromo dynamic model clarifies why a nucleon is bonded only to its nearest neighbors. Corresponding to the meson exchange model of the 1930’s, the residual chromo dynamic model hypothesizes that the nuclear force is due to an exchange of virtual particles. This model is one of the few models of the nuclear force that takes quarks into consideration. However, mathematically, it is very difficult to derive the nuclear force from the quantum chromo dynamics using the Schrödinger equation [40], even for a system of only two nuclides. This difficulty arises because each nucleon consists of three quarks, such that the system of two nucleons is a six-body problem.

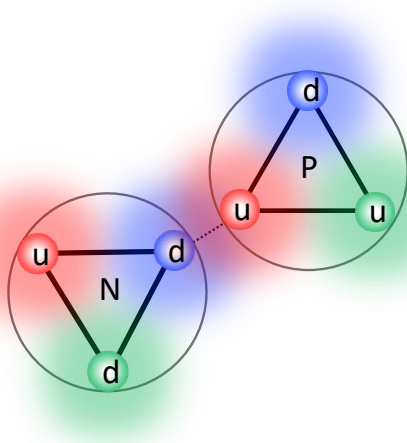


Fig. 1: The nuclear binding of deuterium, as hypothesized by the residual chromo dynamic force

2.11. Electromagnetic Hydrogen Model

An electromagnetic model of the nuclear force was proposed [41], which can accurately give the binding energy for a few of the hydrogen isotopes, but this model has yet to be extended to larger nuclides. It is based on an assumed dipole moment of a bonded neutron (as opposed to a free neutron).

2.12. Model summary

In summary, the current models focus on specific aspects of the nuclear force, most of them relatively secondary behaviors, rather than focusing on the more salient behaviors, such as particle decay. The following is a partial list of some very basic questions that should be answered by a good model. Currently, no one model can answer them all.

- Why do certain medium-sized isotopes, such as ^{150}Dy , exhibit alpha radiation, and yet certain larger isotopes, such as ^{208}Pb , do not?
- Why is ^8Be so extremely unstable, and why does it exhibit alpha radiation?
- Considering the daughter nuclides after the fission of ^{235}U , why is there an extreme double-humped curve?
- Why do certain light isotopes (such as ^4He , ^8Be , ^{12}C , ^{16}O , ^{20}Ne , etc.) have a spike in their binding energy per nucleon?
- Why does ^4He have a zero thermal nuclear cross section?
- Why is ^5He so extremely unstable?
- Why are the magnitudes of quadrupole moments so much larger than any model predicts?
- What causes a nucleus to eject a neutron (aka neutron decay) in certain nuclides?
- What causes proton decay in certain nuclides?
- What causes alpha decay in certain nuclides?
- What causes spontaneous fission in certain nuclides?
- What causes beta-delayed neutron decay in certain nuclides?
- What causes beta-delayed proton decay in certain nuclides?
- What causes beta-delayed alpha decay in certain nuclides?
- What causes beta-delayed spontaneous fission in certain nuclides?

For most of these questions, the current models can not offer any *theoretical* answer, other than to say, “because experimental energy levels allow the transition.” This response is not a valid theoretical answer, and is merely an experimental observation in support of the laws of thermodynamics. However, all of these questions can be answered with a better understanding of electromagnetic forces within the nucleus.

3. Recent Changes in Our Understanding of Nucleons

3.1. Quarks

In 1964, the existence of quarks was proposed independently by Gell-Mann and Zweig [42, 43, 44, 45], changing the concept of the proton and neutron from homogeneously-charged particles to particles having electrical inhomogeneity. A proton is made up of three valence quarks, two up quarks and one down quark. A neutron is also made up of three valence quarks, two down quarks and one up quark. (Other non-valence quarks may exist inside the nucleons.) Up quarks have an electrical charge which is $2/3$ of an elementary charge. Down quarks have a charge which is $-1/3$ of an elementary charge. Since these concepts about quarks were introduced, we now know that the electrical charge and magnetic moments of a nucleon are confined to the quarks, rather than being homogeneously distributed throughout the nucleon. Illustrated in Fig. 2 are three shorthand symbolic representations, showing the up and down quarks, and the electric charges associated with them. In the first representation, the up quarks, in red, have a $++$ charge ($2/3$ of an elementary charge), and the down quarks, in blue, have a $-$ charge ($1/3$ of an elementary charge). The second symbolic shorthand representation shows just the $++$ and $-$ electric charges associated with the quarks. The third symbolic shorthand representation shows just the quarks as red and blue dots. (Please note that the colors in these figures do not relate in any way to the chromo dynamic force.) The magnetic moments of the up quarks are out of the page, and the magnetic moments of the down quarks are into the page; these moments are not shown.

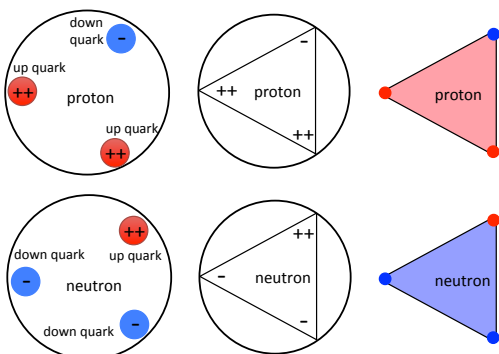


Fig. 2: Three shorthand simplified representations of protons and neutrons.

3.2. Angular Momentum and Mass of Quarks

Prior to the 1980's, particle physicists believed that the spin angular momentum of the quarks was the only contribution to the angular momentum of the proton and neutron. However, experiments proved this concept to be wrong, creating what was

called the nucleon spin crisis. [46, 47, 48, 49, 50, 51].

Further, it was recently learned that the rest mass of the three valence quarks make up a small percentage, approximately 1% or less, of the total mass of a nucleon [52]. Quarks are now considered to be point-like particle, similar to electrons, having no physical dimensions. (Thus in the drawing in Fig. 2, the circles representing the quarks are not meant to represent their actual physical dimensions, nor is the ratio of their radius to the radius of the nucleon meant to be drawn to scale.)

Since mass of the quarks is extremely small, they do not carry much, if any, kinetic energy related to their intrinsic angular momentum. Quarks have an intrinsic spin of $\frac{1}{2}$, but similar to the electron, there is no classical radial speed at which the particle is spinning. In a free nucleon, one that is not bonded inside of a nucleus, it was assumed prior to the 1980's, that the quarks were free to move around with no net orbital angular momentum, and the sum of the spin of the quarks was assumed to be equal to the spin of the nucleon. However, it was found experimentally that the spin of the nucleon is not equal to the sum of the spin of the quarks [46].

Particle physicists now believe there is a net orbital component to the movement of the quarks, rather than random motion. It is currently postulated by particle physicists that the spin of the nucleon, as well as the bulk of its mass, is due to the collective motion of the hundreds of energetic quarks and gluons inside a nucleon. There is another issue concerning these quarks and massless gluons confined within the nucleus, related to uncertainty, forcing the quarks to be extremely energetic. Exacerbating this issue even more, in 2013 as a result of better experimental measurements, the charge radius of the nucleon was corrected to a smaller value of 0.84087 femto-meters [53]. Calculations for the *residual* chromo dynamic model circumvent this issue by using unrealistically large values for the masses of the quarks in their calculations, and then extrapolating down to the more realistic smaller values [54]. (This unrealistically large value used for the quark mass also helps the convergence of the computer solution, but it also creates potentially large errors in the resultant answers.)

Recall that the chromo dynamic force is considered to be large enough to confine and bind together the energetic quarks, despite their energetic vibrating circular motion. Random motion of the quarks inside a bonded nucleus need not be assumed, especially since the orbital angular momentum of the quarks is considered to contribute a significant part of the proton's spin.

3.3. Recent Experimental and Theoretical Progress of the Cluster Model

The recent research regarding the clustering model has shown that clustering structures do indeed exist within nuclei [55, 56, 57, 58, 59, 60], confirming the concept of an actual structure inside a nucleus. Recent research in the clustering structure of nuclides further corroborates the experimentally-observed collective motion of nuclei, strongly suggesting that nucleons do not move independently inside a nucleus. Clustering is observed as a general phenomena at high excitation energies in light alpha-like nuclei, and clustering is a general feature not only observed in light neutron-rich nuclei, but also in less common systems, such as ^{11}Li and ^{14}Be [23]. The alpha-cluster model has now been extended beyond just the alpha nuclei, with much study and research in the field of cluster structure and of so-called "nuclear molecules". These "nuclear molecules" can be thought of as being built from building blocks or segments, which are linked together to form chain-like structures, called "nuclear molecules."

These nuclear molecule are illustrated graphically in Ikeda diagrams [60]. A sample of Ikeda diagrams are shown in Fig. 3, to familiarize the reader with this type of diagram for nuclear structure.

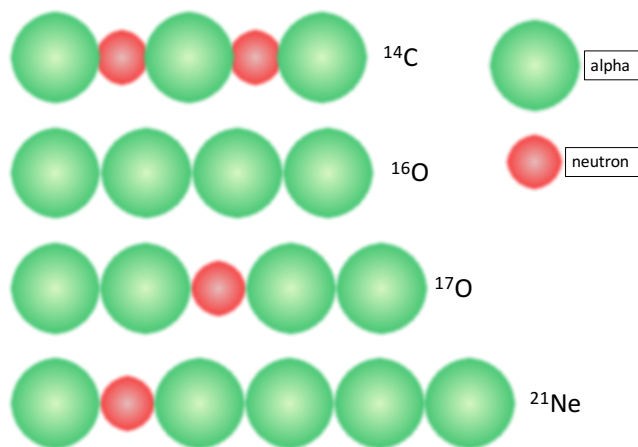


Fig. 3 Ikeda diagrams of four simple nuclides

As can be seen from the Ikeda diagrams, the nuclear segments form chain-like configurations, to create the nuclear molecules of the nucleus. Again, this is long chain-like shape is verified both experimentally and theoretically within the Nuclear Cluster Model. (It is possible that this chain-like shape curls up to form a more elliptical overall shape, like a coiled chain.)

4. A Slight Conceptual Change to the Residual Chromo Dynamic Force

The *residual* chromo dynamic force postulates that the nuclear force is a residual effect of the chromo dynamic force and the “color charge” of the quarks. The *residual* chromo dynamic force is postulated to be an exchange of pions between the quarks of different nucleons. However, one simple extension to this hypothesis makes an interesting difference in our understanding of the forces involved within the nucleus. If this force is dependent upon the up/down polarity of quarks, rather than the color charge of the quarks, then many questions can immediately be answered. The concept here is that a down quark is attracted to an up quark, but not to another down quark. Similarly, an up quark is attracted to down quark, but not to another up quark. The nuclear force is then simply the attraction of the up quark in one nucleon to the down quark in another nucleon--an inter-nucleon force between two quarks. When a bond is made between these two different quarks in two different nucleons, the nucleons themselves are thus bonded, and the nucleus is at a lower overall energy than the sum of the constituent parts. (Thus, it has a higher binding energy.)

This simple change of concept, that the nuclear force is dependent upon the up/down polarity rather than the color charge of the quark, easily explains why a system of 6 protons and 6 neutrons is at a lower energy (and at a higher binding energy) than 5 protons and 7 neutrons. It is because 6 protons and 6 neutrons can form one bond for every pair of up-down quarks. There are 18 up quarks and 18 down quarks in the system of 6 protons and 6 neutrons, thus there could be 18 pairs of up-down quarks, and 18 bonds. However, for 5 protons and 7 neutrons, there are 19 down quarks and 17 up quarks, thus only 17 bonds could be formed. The nucleus with 5 protons and 7 neutrons would be at a higher overall energy (and at a lower binding energy) than the system of 6 protons and 6 neutrons. With this simple change, we can also now understand why a nucleon can only bond to its nearest neighbors. Specifically, a nucleon can only bond to three other nucleons because it only has three valance quarks with which to bond. The quarks involved in the bonding must be of opposite up/down polarity. This single concept immediately explains the asymmetry force of the Weizsäcker formula, because the greatest number of bonds occurs when there are equal numbers of up quarks and down quarks, which in turn means an equal number of protons and neutrons.

This new concept explains why there is a limited number of bonds for each nuclide in the nucleon, clarifying in a definitive explanation the first term of the Weizsäcker formula. Also, as a direct result, there is a definitive explanation of the asymmetry force--because unequal numbers of neutrons and protons form fewer bonds. The Coulomb energy term of the Weizsäcker formula is also easily explained as being related to the electrical energy of the net positive charges. For this one simple change in the residual chromo dynamic model, we can understand three of the five terms of the Weizsäcker formula as being a direct results of the quark-to-quark inter-nucleon binding. Thus, this simple variation of the residual chromo dynamic force, based on up-to-down polarity rather than color charge, associates the residual chromo dynamic model with the conceptual terms of the semi-empirical Weizsäcker formula.

Quick calculations have been made to test this hypothesis. [61] These calculations show that this concept of inter-nucleon up-to-down quark bonding reproduces the binding energy curve surprisingly well, using only one variable—the strength of the bond. Such good replication, achieved with simple mathematics, points toward the correctness of this concept. The quick calculation of this concept did not assume any particular type of force for the bond; it only assumed that a bond was formed between an up quark and a down quark. If the electromagnetic force is assumed to be the force between the up and down quarks, then a more rigorous and detailed calculation can be done; this is the topic to be explored in this paper.

First, a brief review of the electromagnetic force is given.

4.1. Electromagnetic Forces within a Nucleus

As outlined above, if the residual chromo dynamic force is related to the up/down quark polarity, (such that a bond can form between an up quark in one nucleon to a down quark in another nucleon), then this simple concept explains many aspects about nuclear behavior in an understandable manner.

Recall that the electrical charges and magnetic moments of the nucleons are contained within the quarks. Due to the inverse-square-law dependence with distance for this force, the electromagnetic forces between an up quark and a down quark can be extremely strong, if they are close enough. The purpose of this paper is to determine if the electromagnetic forces can be sufficiently strong to hold the nucleons together in the nucleus.

Shown in Fig. 4 is a representation of an electromagnetic bond.

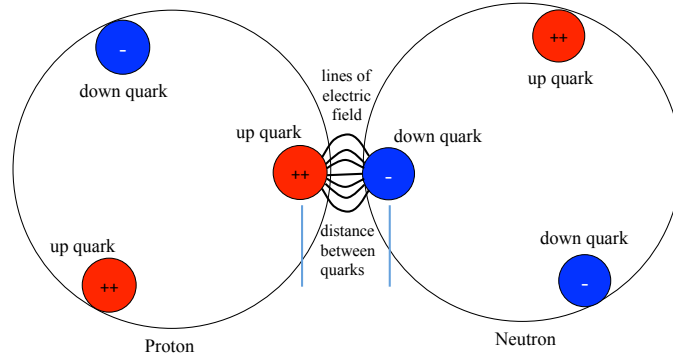


Fig. 4: The electromagnetic bond between quarks.

In other words, the force binding these two nucleons is the electromagnetic force between the quarks.

4.2. Brief Review of the Electric Energy

The electric energy [62,63,64,65] between two electrically charged particles is shown in equation (1), where r_{12} is the distance between particles 1 and 2, and q_1 and q_2 are the charges on particles 1 and 2, respectively. U_{E12} is the electric energy.

$$U_{E12} = \frac{-q_1 q_2}{((4\pi\epsilon)_0)(r_{12})} \quad (\text{Eq. 1})$$

For additional charges, the electrical energies are simply summed for every pair of charges, as shown in equation (2).

$$U_{electric\ total} = \sum_{i=1}^{n-1} \sum_{j=i+1}^n \frac{-q_i q_j}{((4\pi\epsilon_0)(r_{ij}))} \quad \text{Eq. (2)}$$

4.3. The Magnetic Energy

The magnetic energy [66, 67, 68, 69, 70, 71, 72] between two magnets is more complicated than the electric energy because it has vector and position dependence. Given two magnets, with magnetic moments μ_1 and μ_2 , the magnetic field of magnet₁ must be determined at the location of magnet₂. This magnetic field is symbolized as B_{12} . The resultant energy, $U_{magnetic12}$, is the negative dot-product of the vector μ_2 with the vector B_{12} , as shown in equation (3).

$$U_{magnetic12} = -\vec{\mu}_2 \cdot \vec{B}_{12} \quad \text{Eq. (3)}$$

For a collection of magnets, the total magnetic energy is the double summation over all magnet pairs, as shown in equation (4).

$$U_{magnetic\ total} = \sum_{i=1}^{n-1} \sum_{j=i+1}^n -\vec{\mu}_i \cdot \vec{B}_{ij} \quad \text{Eq. (4)}$$

where \vec{B}_{ij} is the vector magnetic field established by the i^{th} magnet at the location of the j^{th} magnet.

The equation for \vec{B}_{ij} is:

$$\vec{B}_{ij} = \frac{\mu_0}{4\pi} \left\{ \frac{3(\vec{\mu}_j \cdot \vec{r}_{ij})\vec{r}_{ij} - r_{ij}^2(\vec{\mu}_j)}{r_{ij}^5} \right\} \quad \text{Eq. (5)}$$

Due to the vector properties of this energy, the lowest energy configuration for two magnets is a stacked bond, in which the magnetic moments of the magnets are aligned, in a stacked orientation with respect to each other, and as close as physically possible. Another way for two magnets to bond is a side-by-side bond, with the magnetic moments anti-parallel, oriented side-by-side, and as close as physically possible. An angled bond, in between a stacked and a side-by-side bond, will give intermediate results.

Combining equations 2, 4, and 5, we see that the total electromagnetic energy of a distribution of charges and magnets is shown in equation (6).

$$U_{EM\ total} = \sum_{i=1}^{n-1} \sum_{j=i+1}^n \frac{-q_i q_j}{(4\pi\epsilon_0)(r_{ij})} + \sum_{i=1}^{n-1} \sum_{j=i+1}^n \frac{-\mu_0}{4\pi} \left\{ \frac{3(\vec{\mu}_j \cdot \vec{r}_{ji})(\vec{\mu}_i \cdot \vec{r}_{ji}) - r_{ji}^2(\vec{\mu}_i \cdot \vec{\mu}_j)}{r_{ji}^5} \right\} \quad Eq. (6)$$

From quantum field theory we know that quarks behave like point-like Dirac particles, each having their own inherent magnetic moment, rather than having a magnetic moment caused by a current loop of spinning charge [73, 74].

4.4. The Limitation of the Electromagnetic Force

Prior to the 1960's, the proton was incorrectly thought to be homogeneously charged and to have a radius of about 1.2 fm. As a result, the strongest electrical energy between two such protons was thought to be $9.6 \cdot 10^{-15}$ Joules.

The energy required to free a single nucleon from a nuclide is experimentally much larger than this. For this reason, the nuclear force was believed to be much stronger than the electric force. As a result, this incorrect concept of a homogeneously charged proton created an incorrect limitation of the electric force. Unfortunately, this incorrect concept is still often perpetuated even today, completely ignoring the electrical characteristics of quarks.

If the minimum quark-to-quark distance (defined as the minimum distance of one quark in one nucleon to a second quark in another nucleon) is 1/10 the radius of a proton, the electrical energy between the two quarks is $6.1 \cdot 10^{-13}$ Joules. This value is made even larger by including the magnetic energy. Mathematically, in the limit as the distance goes to zero, the electromagnetic energy goes to infinity. Hence, the electromagnetic energy can be extremely large if the quarks are close enough to each other. Since the charge of the nucleons resides within the quarks, it is obvious that a quark from one nucleon could bond electromagnetically with a quark in another nucleon, and that the resultant electromagnetic force between two such quarks can be extremely large.

4.5. Short-Range versus Long-Range Forces

Since there is no indication of a nuclear force at large distances, it was previously thought that the nuclear force must be a short-range force. Due to the misconception that protons were homogeneously charged, it was thought that the electromagnetic force could not be same as the nuclear force; thus the existence of a force, different from the electromagnetic force, was postulated. Given the understanding that the nuclear force is electromagnetic, the requirement of a short-range force is no longer necessary.

4.6. Brief Review of the Nuclear Electric Quadrupole Moment

The electric quadrupole moment of a distribution of charge is a frequently misunderstood topic that deserves review before proceeding [75, 76, 77].

A monopole moment is the net charge of an object, assuming the object has a spherical distribution of charge with radial symmetry. Any distribution of charge with radial symmetry will have only an electric monopole moment. If the distribution has a polarity of positive and negative charges, then the object will also have an electric dipole moment. If the distribution of charge has an ellipsoidal shape, instead of a spherical shape, then the object will have an electric quadrupole moment. The quadrupole moment is related to the eccentricity of the charge distribution, and it can be either prolate (positive, cigar shaped) or oblate (negative, pancake shaped). The quadrupole moment of a non-spinning object is referred to as its "intrinsic" quadrupole moment, and this moment is different from the "measured" quadrupole moment, if the object is spinning.

If a *prolate* object (with an intrinsic quadrupole moment Q_0) is spinning, then depending on the axis of spin, the measured quadrupole moment may be smaller than the intrinsic quadrupole moment, and it can even be negative. However, the measured quadrupole moment can not be larger than the intrinsic quadrupole moment. Thus for an intrinsically prolate charge distribution, the measured quadrupole moment can be smaller in absolute value than the intrinsic quadrupole moment, and it can be either positive or negative. It can not be larger in absolute value.

Correspondingly, if an *oblate* object (with an intrinsic quadrupole moment $-Q_0$) is spinning, then depending on the axis of

spin, the measured quadrupole moment can be smaller in absolute value, all the way to zero. The measured quadrupole moment can not be positive, and it can not have a larger absolute value than the intrinsic quadrupole moment. Thus, for an intrinsically oblate charge distribution, the measured quadrupole moment can be smaller in absolute value than the intrinsic quadrupole moment, and it can be either zero or negative.

To reiterate, the absolute value of the measured quadrupole moment of a spinning object can never be larger than the absolute value of the intrinsic quadrupole moment. *Thus, if a nuclear model predicts a small intrinsic quadrupole moment, smaller than the measured quadrupole moment, then this model is inherently flawed and incorrect.* Conversely, if a nuclear model predicts a large intrinsic quadrupole moment, one that is larger than the measured quadrupole moment, then this can easily be explained as being due to the angle of the spin axis.

Taken into the quantum realm, similar principles apply. The measured quadrupole moment, Q_{measured} , is related to the intrinsic quadrupole moment, $Q_{\text{intrinsic}}$, as shown in equation (7)

$$Q_{\text{measured}} = Q_{\text{intrinsic}} \left(\frac{3K^2 - J(J+1)}{(J+1)(2J+3)} \right) \tag{Eq. (7)}$$

where K is the projection of the spin axis onto the symmetry axis and J is the total spin of the nucleus [76].

There is a common misconception that large quadrupole moments only exist in isolated sections of the nuclear table; however, the data for nuclear quadrupole moments and the nuclear deformation parameters show that this concept is not true. Fig. 5a shows all the experimental quadrupole moments for all nuclides from $A=0$ to 250 for those nuclides with a spin. The blue line in Fig 5a shows the predicted maximum quadrupole moments of the shell model. (All data for Fig. 5a extracted from reference [78].)

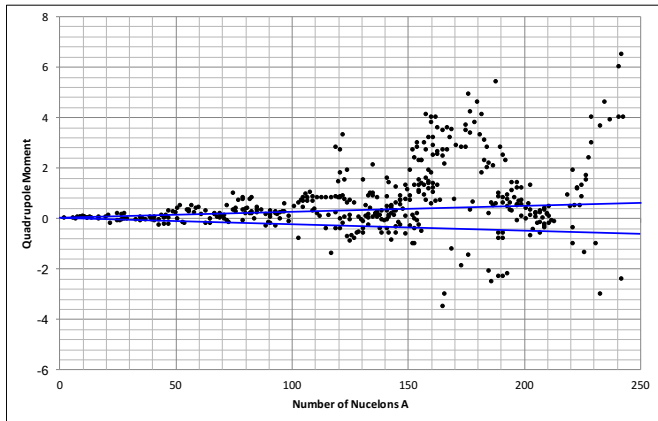


Fig. 5a: Experimental quadrupole moment. The predicted maximum quadrupole moment of the shell model is shown by the blue lines.

Fig. 5b shows the quadrupole moments for the nuclides with even-even values of Z and N , all of which have 0 spin. In Fig. 5b note that all of these quadrupole moments are much larger than what the shell model can explain, which is again indicated by the blue line. (All data for Fig. 5b are extracted from reference [79].)

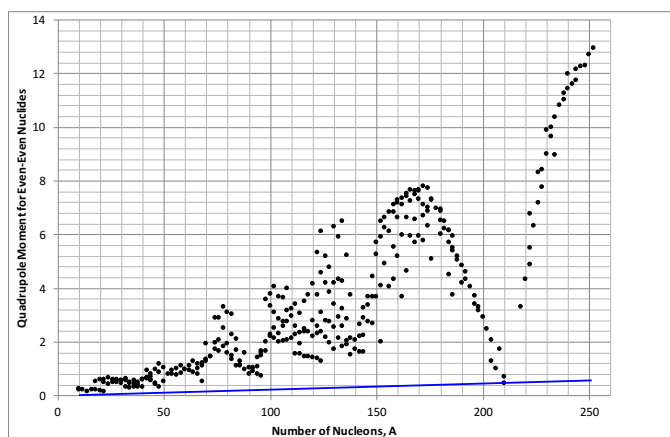


Fig. 5b: Experimental quadrupole moment of even-even nuclides. The predicted maximum quadrupole moment of the shell model is shown by the blue line.

A quantity similar to the quadrupole moment is the deformation parameter. Fig. 5c shows all the experimentally known deformation parameters. If the shell model were correct, then all of the deformation parameters seen in Fig. 5c should be less than one, indicated by the blue line. However, they are much higher. (All data for Fig. 5c extracted from reference [79].)

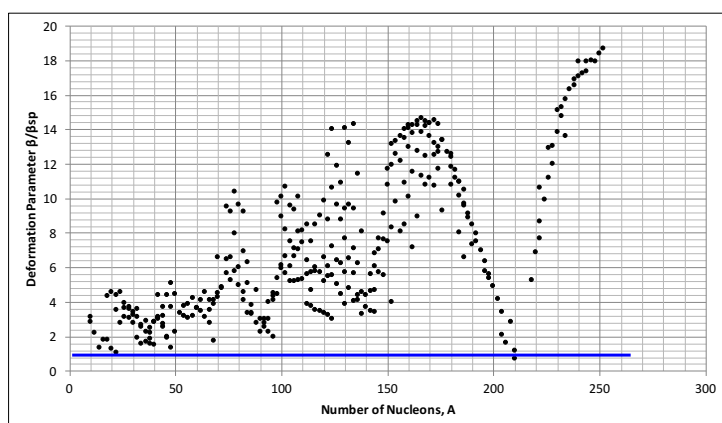


Fig. 5c: The ratio of the experimental nuclear deformation parameter divided by the predicted deformation parameter of the shell model, indicated by the blue line at the value 1.

As can be seen, the quadrupole moments and the deformation parameters are much larger than the shell model can explain. As shown in Fig. 5a, 5b, and 5c, almost all nuclei have a quadrupole moment and deformation parameter that are much larger than what the shell model can explain. The distortion is not just in a few isolated regions of the nuclear table, but covers the entire range. The large experimentally-measured quadrupole moments for the vast majority of nuclides negates any concept of spherical nuclides. These large quadrupole moments are in direct conflict with any model that pre-assumes a spherical shape.

With the exception of analyzing quadrupole moments, presently when researchers interpret the data from an experimentally probed nucleus, the shape of the nucleus is pre-assumed to be a spherical shape. Then, for this pre-assumed spherical shape, the best value of its radius R is forced-fit to the data, without any attempt to examine a different shape [80,81,82]. For example, the interpretation of the electron scattering data only considers the electric monopole moment. The interpretation of this data is then normalized over the charge density to force-fit the charge inside a sphere. A Gaussian curve is assumed as the skin of the nuclide. So regardless of the actual shape, the forced-fit normalized data makes the nucleus appear to be spherical in shape with a Gaussian skin. Even the so-called model-independent interpretations of scattering data still assume a spherical shape [83]. The experimental data is force-fit to be spherical to match the models, and most of the current nuclear models pre-assume a spherical shape, perpetuating the misconception regarding a spherical nucleus. As can be readily seen in Fig. 5, there is very little experimental justification for a spherical shape.

4.7. The Schrödinger Equation

The Schrödinger equation [84] is a useful tool and has been successful in many areas of quantum physics, especially for the

behavior of atomic electrons. The Schrödinger equation is a second-order differential equation that can only be solved for a given potential energy, kinetic energy, and initial conditions. Thus it is inherently difficult to use. Previous nuclear models have tried to model the nuclear potential, using different formulas for the Hamiltonian to obtain the probability function of the particle in question. However, the Schrödinger equation has proven to be extremely difficult and almost intractable to use for the nuclear force, especially for large nuclides.

If the Schrödinger equation is to be used properly for the nuclear force, the correct solution can only be obtained if the Hamiltonian is related to the electromagnetic energy of each individual quark in the nuclide. The proper potential energy well must take into account an energy that can be both attractive and repulsive, as well as taking into account the vector properties of the energy. However, even without polarity and vector dependence, the quark-based solution for even ^2H has proven to be extremely difficult [28]. Fortunately the electromagnetic equations are more easily applied.

4.8. The Concept of a Nuclear Bond Similar to an Atomic Bond

For the electromagnetic model, the nuclear bond is an energy well between the two quarks forming the bond. The energy well is between the up quark of one nucleon and the down quark of another nucleon. It is this bond between the quarks that lowers the overall energy of the nucleus. This aspect is similar to the electronic bonds between the atoms of a molecule. In atomic bonding, one atom can not bond to an indefinite number of other atoms. Similarly, one nucleon can not bond to an indefinite number of other nucleons. Rather the number of bonds is limited by the number of quarks available for bonding. Thus each nucleon, with only three valence quarks, can only bond to three other nucleons. Two quarks are needed for one bond.

4.9. Summary of the Electromagnetic Force within the Nucleon

The following is a review of the basic concepts for the proposed electromagnetic model.

- The electromagnetic force is valid inside the nucleon.
- The electric charge and the magnetic moment of the nucleons are contained within the quarks.
- The quarks of the nucleons have a spatial quantum probability distribution associated with the nucleon in which they are located. (An equilateral triangle is assumed for simplicity.)
- There are three possible bonds per nucleon, one for each valence quark. After three bonds, the nucleon can not bond to a fourth nucleon.
- A pair of quarks, one from two different nucleons, is needed for one bond.

All of the above considerations are used in this electromagnetic model, along with the following quantum considerations:

- The kinetic energy of the quantum angular momentum of the nucleus [85, 86, 87] is also properly taken into account. (Note that this kinetic energy of the nuclear angular momentum strongly correlates to the energy of the pairing term in the Weizsäcker formula.)
- The lowest energy configuration is assumed for the ground state.
- There is a minimum distance between two quarks of two different nucleons, consistent with the Pauli Exclusion principle and the hard core repulsion.
- The hard core repulsion of the nucleons prevents any given nucleon from bonding more than once to another given nucleon. Any nucleon that attempts to bond twice to another nucleon is involved in a “double-nucleon bond”. A double-nucleon bond is not allowed; an attempted “double-nucleon bond” will break both bonds.
- A quark that attempts to bond to more than one other quark is engaged in a “triple-quark bond”. This triple-quark bond is not allowed, and an attempted triple-quark bond will break the bonds.

5. The Nuclear Configurations of the Lowest Energy States

For every nuclide in this paper, the position of each quark is defined in a matrix with xyz spatial coordinates and an electric charge value of either $-1/3$ or $+2/3$ of an elementary charge. The value of the magnetic moment, for either the up or down quark, and the three dimensional vector direction of each magnetic moment for each quark are also included in the matrix. Stacked magnetic bonds, angled magnetic bonds, or side-by-side magnetic bonds are determined, depending on the physical constraints of the configuration. Every nuclide in this paper is placed into its lowest energy state in accordance with the rules for electromagnetic energies and the electromagnetic equations. Double-nucleon bonds or triple-quark bonds are not allowed, due to the hard core repulsion of the nucleons. This matrix file is used to calculate the change in the electromagnetic energy from the original constituent parts, and the result is then used to calculate the nuclear binding energy.

Here are some simple considerations to recognize when the nucleons form into segments.

- When a bond is formed the net charge of the bond is $+1/3$ of an elementary charge. This net positive charge is present at every bond.
- The nucleons cluster into segments, similar to the segment clusters described in the cluster model. This clustering is due to

the electromagnetic force situating the nuclide into its lowest energy configuration.

- Due to the consideration that the nucleons can only bond three times, the nucleons will tend to cluster into alpha particle segments, each segment consisting of two protons and two neutrons. A segment consisting of two protons and two neutrons is the dominant type of segment, and is called an alpha segment.
- Another type of segment that is possible is a tri-nucleon segment consisting of one proton and two neutrons, called a tritium segment.
- Another type of segment that is possible is a tri-nucleon segment consisting of two protons and one neutron, called a He3 segment.
- Another segment is made of one neutron, called a single-neutron segment.
- Another segment is made of one proton, called a single-proton segment.
- Another segment is made of one proton and three neutrons, called an H4 segment.
- In the lowest energy state, each segment can bond only to one or two other segments.

5.1. Basic Pattern for the Configurations of Stable Nuclides with $A \geq 12$

The electromagnetic model has successfully computer simulated both stable and unstable nuclides, all the way up to californium ^{250}Cf , using only the electromagnetic equations and the equations for quantum angular momentum. From carbon ^{12}C upwards, the stable nuclides follow a relatively simple pattern. This basic pattern is *not* mere speculation, but rather the pattern is due to the lowest energy configuration of the nucleons, when taking into consideration the laws of electromagnetics. The pattern is as follows:

- There is one alpha particle segment for every two protons and two neutrons.
- An open alpha particle segment is in the middle of the configuration. This open alpha particle segment has two unbonded down quarks, and the negative charge of the unbonded down quarks offsets the high Coulomb energy in the middle of the nuclide. It also allows the net positive charge of the nuclide to be spread out a bit further.
- When there are more neutrons than protons, and Z is even, then the extra neutrons are single neutron segments, interspersed between the alpha segments.
- When Z is odd, and there are one or two more neutrons than protons, then the odd proton combines with the two extra neutrons to form an H3 segment. (An H3 segment is comprised of two neutrons and one proton.)
- If there are enough extra neutrons, then three of the extra neutrons will bond with a proton to form an H4 segment. This bonding pattern will occur only once for odd Z , and only twice for even Z . These H4 segments are on the end of the configuration.
- When there is an equal number of protons and neutrons, and this number is odd, such as nitrogen ^{14}N , then there is a single neutron segment plus a single proton segment. This situation occurs infrequently in the stable nuclides, but more frequently in the unstable nuclides.

5.2. Basic Pattern for the Radioactive Nuclides

For the radioactive nuclides, there are two more considerations for their lowest energy configurations. Again, these patterns are not mere speculation, but rather the patterns emerge as a direct result of the electromagnetics energies.

- When there are more protons than neutrons, then the one extra proton will form either a single proton segment or an He3 segment. (A He3 segment is comprised of one neutron and two protons.)
- Any nuclide with more single neutron segments than alpha segments will double-up the single neutron segments in pairs, without an alpha segment between them. These doubled-up single neutron segments tend to be near the middle of the nuclide. There are no stable nuclides with doubled-up neutron segments in the ground state.

5.3. Particle Decay

Particle decay is defined as alpha decay, neutron decay, proton decay, spontaneous fission, and the beta-delayed reactions of the same. An in-depth analysis of the electromagnetic causes of particle decay will be covered in subsequent papers of this series. Briefly stated, in the smaller nuclides, all particle decay occurs when the electromagnetic force within the nuclide pulls or pushes on the unbonded quarks in such a way as to cause either a double-nucleon bond or a triple-quark bond—both of which are not allowed. If the energy transference is large enough when there is an attempt to form either of these prohibited bonds, then the bonds will break and particle decay results.

The alpha decay exhibited by the larger nuclides, $A > 150$, is a statistical mechanism, different from the near-instantaneous alpha decay seen in the smaller nuclides. The alpha decay of the larger nuclides is a topic that will be covered in subsequent papers of this series. Briefly, the mechanism is similar to Gamow's model of alpha decay for the larger nuclides, in that it is dependent on random statistical parameters. However, the electromagnetic model can predict the half life of alpha decay, based on *theoretical* parameters rather than simply correlating two experimentally-observed parameters. The likelihood of alpha decay is correlated to the strength of the net repulsive electric energy seen by the end-most alpha-particle segment in the

configuration.

5.4. The Smaller Nuclides, A<12

The nuclides smaller than ¹²C cannot follow the pattern outlined above, simply because they do not have enough nucleons to do so. Also, the energy of the quantum angular momentum is a much larger percentage of the overall energy for the lighter nuclides. Both of these characteristics contribute to the more unusual nuclear behaviors of the smaller nuclides. An in-depth analysis of the nuclear behaviors of the smaller nuclides, A<12, is covered in subsequent papers of this series.

6. An Example Calculation for ²H

For every nuclide in this paper, the position of each quark is defined in a matrix with xyz spatial coordinates and an electric charge value of either -1/3 or +2/3 of an elementary charge. For example, the nuclide of ²H is composed of one proton and one neutron, with three quarks in each nucleon, for a total of 6 quarks, three up quarks and three down quarks. Within each nucleon, the quarks form an equal-lateral triangle. Using the symbolic shorthand representations similar to those shown in Fig. 1 and 2 the configuration for the example for ²H is shown in Fig. 6. Note in Fig. 6 the distance between two internucleon quarks is 2.11083×10^{-16} meters, and the separation of the quarks in the nucleon is 1.27385×10^{-15} meters. The radius of the nucleon is 0.841×10^{-15} meters. The orientation of the xyz coordinate system is also shown. Listed in Table 1 are the name of the quark, the (x,y,z) location coordinates in meters, the quark value in units of elementary charge, the magnetic dipole vector, and the magnetic dipole moments in units of nuclear magnetons.

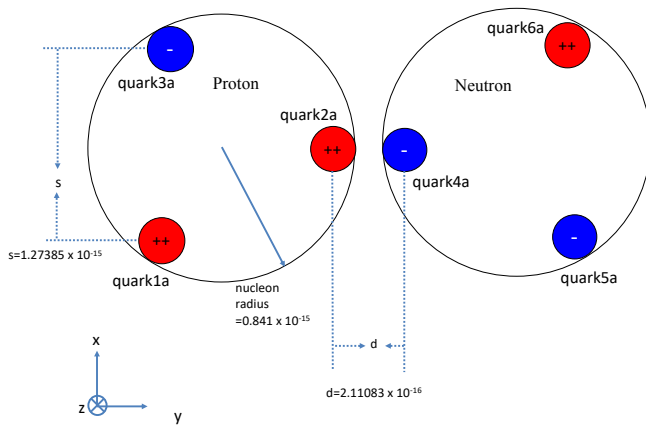


Fig. 6: Short-hand simplified graphic of ²H.

Quark name	Quark location	Quark value	Magnetic vector	Magnetic dipole moment
quark1a	(0, 0, 0)	0.666	(0, 0, 1)	1.85
quark2a	(6.36926×10^{-16} , 1.10319×10^{-15} , 0)	0.666	(0, 0, 1)	1.85
quark3a	(1.27385×10^{-15} , 0, 0)	-0.333	(0, 0, -1)	-0.97
quark4a	(6.36926×10^{-16} , 1.31427×10^{-15} , 0)	-0.333	(0, 0, -1)	-0.97
quark5a	(0, 2.41745×10^{-15} , 0)	-0.333	(0, 0, -1)	-0.97
quark6a	(1.27385×10^{-15} , 2.41745×10^{-15} , 0)	0.666	(0, 0, 1)	1.85

The bond is between quark2a and quark4a. The vector orientation of magnetic bond is a side-by-side bond, with the up quark magnetic moment going into the page, and the down quark magnetic moment going out of the page.

6.1. An Example of the Electric Energy Calculation

The electric energy of this configuration is calculated using equation 2, the double summation. For 6 quarks, the summation includes 15 terms, where each U_{Eij} term represents the electric energy between the i^{th} and j^{th} quark.

$$U_{electric_total} = U_{E12} + U_{E13} + U_{E14} + U_{E15} + U_{E16} + U_{E23} + U_{E24} + U_{E25} + U_{E26} + U_{E34} + U_{E35} + U_{E36} + U_{E45} + U_{E46} + U_{E56}$$

To fill in these values we use Eq. 1, using the number values from Table 1, and solving for the r_{ij} value first:

$$r_{12} = \text{Sqrt}[(6.36926 \times 10^{-16} - 0)^2 + (1.10319 \times 10^{-15} - 0)^2 + (0 - 0)^2]$$

$$r_{12} = 1.27385 \times 10^{-15} \text{ meters}$$

Using this value of r_{12} to solve for the electrical energy from quark 1 to quark 2:

$$U_{E12} = (-1)(8.98755 \times 10^9)(2/3)(2/3)(1.602 \times 10^{-19})^2 / (1.2738 \times 10^{-15})$$

$$U_{E12} = -8.04935 \times 10^{-14} \text{ joules}$$

The negative sign denotes that it is a repulsive energy. The other values are similarly calculated:

$$U_{E13} = +4.02468 \times 10^{-14}$$

$$U_{E14} = +3.5104 \times 10^{-14}$$

$$U_{E15} = +2.12076 \times 10^{-14}$$

$$U_{E16} = -3.75243 \times 10^{-14}$$

$$U_{E23} = +4.02468 \times 10^{-14}$$

$$U_{E24} = +2.42883 \times 10^{-13}$$

$$U_{E25} = +3.5104 \times 10^{-14}$$

$$U_{E26} = -7.02079 \times 10^{-14}$$

$$U_{E34} = -1.7552 \times 10^{-14}$$

$$U_{E35} = -9.38107 \times 10^{-15}$$

$$U_{E36} = +2.12076 \times 10^{-14}$$

$$U_{E45} = -2.01234 \times 10^{-14}$$

$$U_{E46} = +4.02468 \times 10^{-14}$$

$$U_{E56} = +4.02468 \times 10^{-14}$$

The sum of this electric energy is 2.70207×10^{-13} joules. Notice that the dominant contribution to this energy is from the bond seen at U_{24} . This is the electric energy after a nucleus is formed from a proton and a neutron. However, in order to properly calculate the bonding energy, the electric energy before the proton and neutron forms a nucleus must be subtracted from this sum. In other words, the energy of all the individual isolated protons and neutrons must be subtracted from this sum. The electric energy of one individual isolated proton is:

$$U_{E12} + U_{E13} + U_{E23} = 0 \text{ joules}$$

The electric energy of one individual isolated neutron is:

$$U_{E45} + U_{E46} + U_{E56} = 6.03701 \times 10^{-14} \text{ joules}$$

This then gives the net electric energy as $U_{\text{net electric energy}} = (2.70207 \times 10^{-13}) - (6.03701 \times 10^{-14}) = 2.0984 \times 10^{-13}$ joules. This value is used below in the calculation for total binding energy. As seen by the sign, it is an attractive force and an attractive energy.

6.2. An Example of the Magnetic Energy Calculation

Now the magnetic energy for this configuration of quarks must be calculated, using Eqs. 3, 4, and 5. This involves vector math.

$$U_{\text{magnetic total}}$$

$$U_{\text{magnetic_total}} = U_{M12} + U_{M13} + U_{M14} + U_{M15} + U_{M16} + U_{M23} + U_{M24} + U_{M25} + U_{M26} + U_{M34} + U_{M35} + U_{M36} + U_{M45} + U_{M46} + U_{M56}$$

Here U_{Mij} now represents the magnetic energy between the i^{th} quark and the j^{th} quark.

To do this calculation, the magnetic field of the i^{th} quark must be calculated in the vicinity of the j^{th} quark, must be calculated first, using equation 5 and vector math. For this example, we will calculate U_{M14} . From Table 1, the vector values for μ_1 , μ_4 , and r_{14} are:

$$\mu_1 = (0, 0, 9.34407 \times 10^{-27})$$

$$\mu_4 = (0, 0, -4.899 \times 10^{-27})$$

$$r_{14} = (6.36926 \times 10^{-16}, 1.31427 \times 10^{-15}, 0)$$

Plugging this value into Eq. 5, to find the magnetic field vector, yields:

$$\mathbf{B}_{14} = (0, 0, 1.57273 \times 10^{11})$$

Plugging this vector into Eq. 4, yields:

$$U_{M14} = +1.46957 \times 10^{-15} \text{ joules}$$

Here, the positive sign denotes that it is an attractive energy. The other values are similarly calculated. listed below:

$$\begin{aligned} U_{M12} &= -4.22392 \times 10^{-15} \\ U_{M13} &= +2.2147 \times 10^{-15} \\ U_{M14} &= +1.46957 \times 10^{-15} \\ U_{M15} &= +3.24037 \times 10^{-16} \\ U_{M16} &= -2.24373 \times 10^{-16} \\ U_{M23} &= +2.2147 \times 10^{-15} \\ U_{M24} &= +4.86762 \times 10^{-13} \\ U_{M25} &= +1.46957 \times 10^{-15} \\ U_{M26} &= -2.8028 \times 10^{-15} \\ U_{M34} &= -7.70534 \times 10^{-16} \\ U_{M35} &= -1.17644 \times 10^{-16} \\ U_{M36} &= +3.24037 \times 10^{-16} \\ U_{M45} &= -1.16122 \times 10^{-15} \\ U_{M46} &= +2.2147 \times 10^{-15} \\ U_{M56} &= +2.2147 \times 10^{-15} \end{aligned}$$

The sum for all of these is $+4.89704 \times 10^{-13}$ joules, which is a net attractive energy. As before with the electric energy, in order to find the magnetic binding energy, we must subtract the magnetic interaction energy of the isolated independent neutrons and protons prior to them being combined in a nucleus. The magnetic interaction energy of a proton is $U_{M12}+U_{M13}+U_{M23}=2.05488 \times 10^{-16}$ and the magnetic interaction energy of a neutron is $U_{M45}+U_{M46}+U_{M56}= 3.30392 \times 10^{-15}$. For the ^2H nucleus, this energy is subtracted from the previously calculated sum of the magnetic energies, and the net magnetic binding energy is:

$$\begin{aligned} U_{\text{net magnetic energy}} &= (+4.89704 \times 10^{-13} \text{ joules}) - (2.05488 \times 10^{-16}) - (3.30392 \times 10^{-15}) \\ U_{\text{net magnetic energy}} &= 4.8623 \times 10^{-13} \text{ joules} \end{aligned}$$

Similar to the net electric energy, the net magnetic energy is dominated by the magnetic energy of quark2a to quark4a, where the bond is located.

6.3. An Example for the Calculation of the Kinetic Energy of the Orbital Angular Momentum

For ^2H , the proton is assumed to be spin $\frac{1}{2}$, and the neutron is assumed to be spin $\frac{1}{2}$ in the same direction, so that the sum of these two spins is 1. The net spin, of spin angular momentum plus orbital angular momentum of ^2H is 1. This gives the orbital spin as a net zero. Thus for this nuclide, the orbital kinetic spin energy is zero.

Had there been a net orbital spin associated with the nuclide, however, the example of how it is calculated is shown. First we must calculate the center of mass in three dimensions, in Eq. 8.

$$\text{Center of mass} = (X_{\text{center of mass}}, Y_{\text{center of mass}}, Z_{\text{center of mass}})$$

where:

$$\begin{aligned} X_{\text{center of mass}} &= \sum_{i=1}^n (X_i)(m_i) \\ Y_{\text{center of mass}} &= \sum_{i=1}^n (Y_i)(m_i) \\ Z_{\text{center of mass}} &= \sum_{i=1}^n (Z_i)(m_i) \end{aligned}$$

(Eq. 8)

where X_i is the x location of nucleon i , and m_i is the mass of nucleon i . Similarly for Y_i and Z_i . The axis of spin goes through the center of mass, at an angle θ with respect to the y-axis. An arm radius, which is defined as the closest distance of that nucleon to the axis of spin, must be found for each nucleon in the configuration of the nucleus. Using simple trigonometry, this arm radius is shown in Eq. 9, for when theta is defined with respect to the y axis.

$$\text{Radius}_{\text{Arm}_i} = \text{Sqrt}[\Delta x_i^2 + (\Delta y_i \sin(\theta) + \Delta z_i \cos(\theta))^2] \quad (\text{Eq. 9})$$

where Δx_i is the X_i minus the $X_{\text{center of mass}}$, for the i^{th} nucleon. Similarly for Δy_i and Δz_i .

At this point, the arm radius is known for every nucleon in the nucleus. Next the spin inertia I_{spin} for each nucleon must be found. The spin inertia is the arm radius squared multiplied by the mass of the nucleon. This is summed together to get the spin inertia of the entire nucleus, as shown in Eq. 10.

$$I_{\text{spin}_i} = (m_i)(\text{Radius}_{\text{Arm}_i})^2$$

$$I_{\text{spin}_{total}} = \sum_{i=1}^n (m_i)(\text{Radius}_{\text{Arm}_i})^2 \quad (\text{Eq. 10})$$

Once the total spin inertial $I_{\text{spin}_{total}}$ is found, the energy of the orbital angular momentum, as shown in Eq. 11 is calculated. One must know the value of the orbital angular momentum, which is denoted by the small letter l .

$$E_{\text{OrbitalAngularMomentum}} = \frac{(l)(l+1)\hbar^2}{2 \times I_{\text{spin}_{total}}} \quad (\text{Eq. 11})$$

This calculation is done for every nucleus with an orbital angular momentum. For smaller nuclides, $A < 12$, this energy can be a considerable of the bonding energy. For medium to large nuclides, this energy is quite small and could be ignored, but it is done for all nuclides regardless in the computer calculations, just to be thorough.

6.4. An Example for the Calculation of the Total Binding Energy

Binding energy reduces the overall energy of the configuration of nucleons in a nucleus. Similarly, it reduces the overall mass nucleus as compared to the constituent nucleons.

Total Binding energy = Electric Binding Energy + Magnetic Binding Energy – Orbital Angular Momentum energy.
For this example,

$$E_{\text{binding}_{total}} = (2.0984 \times 10^{-13} \text{ joules}) + (4.8623 \times 10^{-13} \text{ joules}) - 0$$

$$E_{\text{binding}_{total}} = 4.34452 \text{ MeV.}$$

The total electromagnetic bonding energy is the sum of the electric and magnetic bonding energies. This is $(2.0984 \times 10^{-13} \text{ joules}) + (4.8623 \times 10^{-13} \text{ joules}) = 6.9607 \times 10^{-13} \text{ joules}$, which is 4.34452 MeV. The actual binding energy for ^2H is 2.22476 MeV. Thus, this calculation is high by a couple of MeV.

6.5. Summary of the Calculations for the Total Binding Energy of all the Nuclides

For every nuclide in the paper, every quark is defined in a matrix with its location in three dimensional space, its value, its magnetic moment and the three dimensional vector direction of each magnetic moment, and these detailed calculations are done as shown in this section. Stacked magnetic bonds, angled magnetic bonds, or side-by-side magnetic bonds are determined, depending on the physical constraints of the configuration.

For large nuclides such as lead ^{208}Pb , which has 624 quarks in it, the calculations for the electric and magnetic binding energy are quite complicated and lengthy, requiring large amounts of memory for the computer program to run. Even so, it only takes a matter of minutes to run a large nuclide such as ^{208}Pb . All of these calculations are done for each and every nuclide in this paper. The numbers in the Table 2 and in the graphs of Fig. 7 are not rough estimates or simple guesses. They are the result of detailed and rigorous calculations.

Every nuclide in this paper is placed into its lowest energy state in accordance with the rules for electromagnetic energies and the electromagnetic equations. Double-nucleon bonds or triple-quark bonds are not allowed, due to the hard core repulsion of the nucleons.

Finding the lowest energy configuration for a nuclide requires trial and error to determine which configuration is the lowest energy. For example, for lithium ${}^6\text{Li}$, 26 different configurations were examined to determine what was the lowest energy configuration. In order to determine the lowest energy configuration for a nuclide, several configurations are tried, and the one with the lowest energy is used. The configuration that is used is not something that is selected based on which configuration gives the best answer, but rather it is selected based on which configuration is the lowest energy.

7. Results and Conclusions

Once the lowest energy configurations are found using electromagnetic equations, there remains only one variable to be selected for the best fit to the binding energy data; namely, the minimum distance between the two quarks of the two different nucleons, called the “minimum quark-to-quark distance”. This model has only one variable to determine. The Weizsäcker formula uses five variables and a conditional logic statement to achieve its mathematical curve-fitting. The electromagnetic model of the nuclear force proposed herein is able to get comparable results with only one variable.

Over a thousand different configurations for different nuclides have been computer modeled using this method to calculate the binding energy based on electromagnetics. These include stable and unstable, large, medium, and small, and ground and high energy states. These detailed calculations have been done for every nuclide listed in Table 2. Each nuclide is placed in the lowest energy configuration; then, using this configuration, the electro-magnetic energy is calculated and the binding energy is determined.

The value for the minimum distance between quarks was selected to be 2.11082×10^{-16} meters. It is the only variable that is selected. This value was not selected by trial and error in order to obtain the best fit to the data, but rather it was selected to give close to zero error for ${}^{40}\text{Ca}$, allowing the rest of the nuclides to fit where they would.

Using this value for the minimum distance between quarks, the resulting bonding energy curve is shown in Fig. 7. For comparison, two sets of values are shown: the calculated binding energy, shown in red circles, and the experimental binding energy, shown in blue diamonds. Fig. 7a shows all the points from $A=2$ to $A=208$. Fig. 7b shows only the points from $A=2$ to $A=60$, for ease of viewing the details of this curve. (Note that the binding energies for the stable nuclides with $A=2, 3, 6$ and 7 are more dependent on spin and the angle of the axis of spin.) As can be seen in Fig. 7b, there is excellent agreement in the reproduction of the experimental data. The downward curve for the smaller nuclides is reproduced and the peaks at the alpha particle nuclides are reproduced.

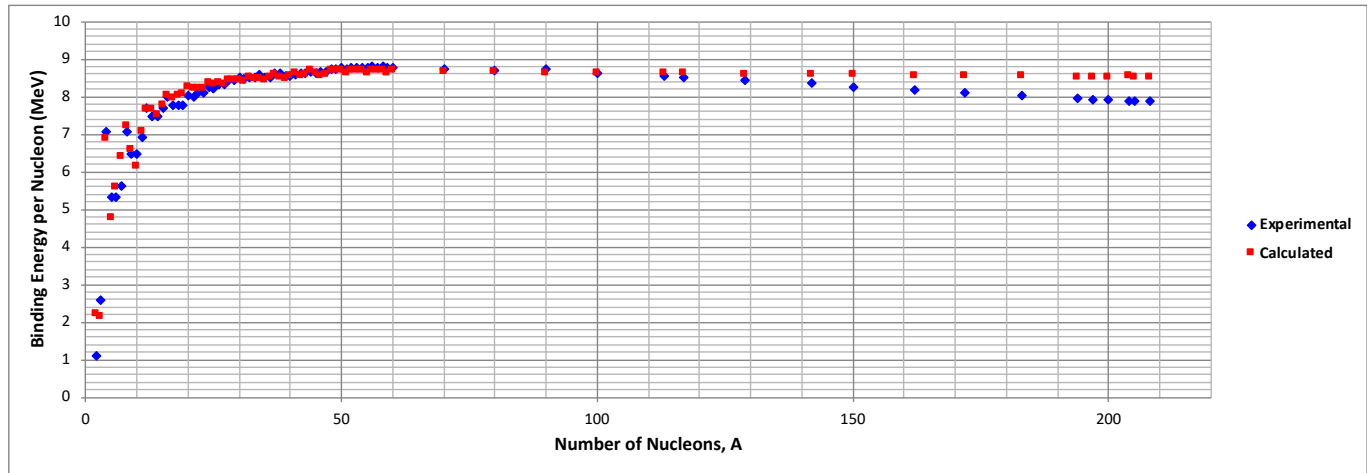


Fig. 7a: Binding energy per nucleon versus A, for both calculated and experimental data, from $A=2$ to $A=208$.

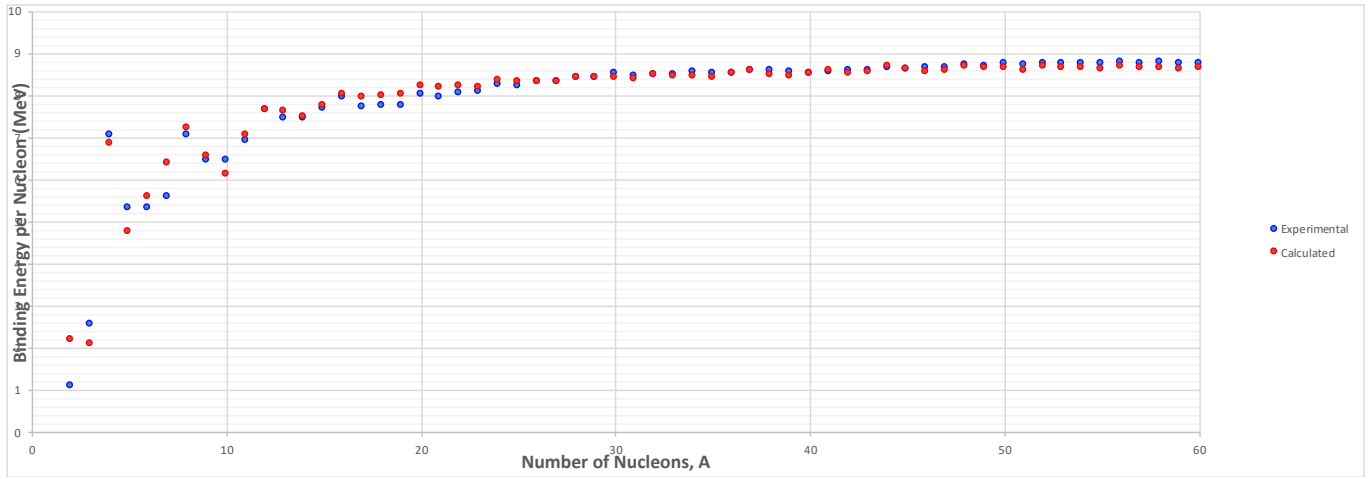


Fig. 7b: Binding energy per nucleon versus A, for both calculated and experimental data, showing detail for the smaller nuclides, from A=2 to A=60.

These data are also presented in Table 2, and show excellent reproduction of the experimental binding energy; most of the nuclides fall within a one or two percent error. For the nuclides with large A, the predicted downward slope is not as severe as is experimentally observed. For these nuclides, the worst error is 8.32% for ²⁰⁴Pb.

TABLE 2
COMPARISON OF EXPERIMENTAL AND CALCULATED BINDING ENERGY

Nuclide	A	Z	N	Experimental Binding Energy, EBE (MeV)	Calculated Binding Energy, CBE (MeV)	% Error	EBE/A	CBE/A
H-2	2	1	1	2.22	4.41318	98%	1.11	2.21
He-3	3	2	1	7.72	6.350778513	17.72%	2.57	2.12
He-4	4	2	2	28.30	27.5109714	-2.77%	7.07	6.88
He-5	5	2	3	26.63	23.84432281	10.45%	5.33	4.77
Li-6	6	3	3	31.99	33.55664463	4.88%	5.33	5.59
Li-7	7	3	4	39.24	44.82377489	14.22%	5.61	6.40
Be-8	8	4	4	56.50	57.7602052	2.23%	7.06	7.22
Be-9	9	4	5	58.17	59.23945254	1.85%	6.46	6.58
B-10	10	5	5	64.75	61.33238839	-5.28%	6.48	6.13
B-11	11	5	6	76.20	77.75612889	2.04%	6.93	7.07
C-12	12	6	6	92.16	91.84852621	-0.34%	7.68	7.65
C-13	13	6	7	97.11	99.46746342	2.43%	7.47	7.65
N-14	14	7	7	104.66	105.1179975	0.44%	7.48	7.51
N-15	15	7	8	115.49	116.4347726	0.82%	7.70	7.76
O-16	16	8	8	127.62	128.5307189	0.71%	7.98	8.03
O-17	17	8	9	131.76	135.4333122	2.79%	7.75	7.97
O-18	18	8	10	139.81	144.2829922	3.20%	7.77	8.02
F-19	19	9	10	147.80	152.8740704	3.43%	7.78	8.05
Ne-20	20	10	10	160.65	164.8561421	2.62%	8.03	8.24
Ne-21	21	10	11	167.41	172.5446382	3.07%	7.97	8.22
Ne-22	22	10	12	177.77	180.8086775	1.71%	8.08	8.22
Na-23	23	11	12	186.56	188.9156486	1.26%	8.11	8.21
Mg-24	24	12	12	198.26	200.6161192	1.19%	8.26	8.36
Mg-25	25	12	13	205.59	208.3377118	1.34%	8.22	8.33
Mg-26	26	12	14	216.68	216.8794256	0.09%	8.33	8.34
Al-27	27	13	14	224.95	224.6324319	-0.14%	8.33	8.32
Si-28	28	14	14	236.54	236.2369786	-0.13%	8.45	8.44
Si-29	29	14	15	245.01	244.4662386	-0.22%	8.45	8.43
Si-30	30	14	16	255.62	252.7252293	-1.13%	8.52	8.42
P-31	31	15	16	262.92	260.5887444	-0.89%	8.48	8.41
S-32	32	16	16	271.78	271.5706273	-0.08%	8.49	8.49
S-33	33	16	17	280.42	279.7819366	-0.23%	8.50	8.48
S-34	34	16	18	291.84	288.1957519	-1.25%	8.58	8.48

Cl-35	35	17	18	298.21	295.667157	-0.85%	8.52	8.45
Ar-36	36	18	18	306.72	306.7118673	0.00%	8.52	8.52
Cl-37	37	17	20	318.78	318.087543	-0.22%	8.62	8.60
Ar-38	38	18	20	327.34	323.4884506	-1.18%	8.61	8.51
K-39	39	19	20	333.72	330.7573498	-0.89%	8.56	8.48
Ca-40	40	20	20	342.05	341.9080812	-0.04%	8.55	8.55
K-41	41	19	22	351.62	352.903988	0.37%	8.58	8.61
Ca-42	42	20	22	361.90	358.8434157	-0.84%	8.62	8.54
Ca-43	43	20	23	369.83	368.8924248	-0.25%	8.60	8.58
Ca-44	44	20	24	380.96	382.3032576	0.35%	8.66	8.69
Sc-45	45	21	24	387.85	388.0794464	0.06%	8.62	8.62
Ti-46	46	22	24	398.19	393.4074295	-1.20%	8.66	8.55
Ti-47	47	22	25	407.07	403.491218	-0.88%	8.66	8.58
Ti-48	48	22	26	418.70	417.0568753	-0.39%	8.72	8.69
Ti-49	49	22	27	426.84	425.5071529	-0.31%	8.71	8.68
Ti-50	50	22	28	437.78	434.0477448	-0.85%	8.76	8.68
V-51	51	23	28	445.84	439.4862366	-1.43%	8.74	8.62
Cr-52	52	24	28	456.34	451.6674486	-1.02%	8.78	8.69
Cr-53	53	24	29	464.29	460.2097234	-0.88%	8.76	8.68
Cr-54	54	24	30	474.01	468.7637783	-1.11%	8.78	8.68
Mn-55	55	25	30	482.08	474.1977824	-1.63%	8.77	8.62
Fe-56	56	26	30	492.26	486.479967	-1.17%	8.79	8.69
Fe-57	57	26	31	499.91	494.9566096	-0.99%	8.77	8.68
Fe-58	58	26	32	509.94	503.2991831	-1.30%	8.79	8.68
Co-59	59	27	32	517.31	508.7045784	-1.66%	8.77	8.62
Ni-60	60	28	32	526.84	520.6395297	-1.18%	8.78	8.68
Ge70	70	32	38	610.52	606.4072667	-0.67%	8.72	8.66
Kr-80	80	36	44	695.44	691.549535	-0.56%	8.69	8.64
Zr-90	90	40	50	783.89	776.6805842	-0.92%	8.71	8.63
Ru-100	100	44	56	861.93	862.4006397	0.05%	8.62	8.62
Cd-113	113	48	65	963.56	972.230688	0.90%	8.53	8.60
Sn-117	117	50	67	995.62	1005.905022	1.03%	8.51	8.60
Xe-129	129	54	75	1087.65	1107.556296	1.83%	8.43	8.59
Nd-142	142	60	82	1185.15	1216.64027	2.66%	8.35	8.57
Sm-150	150	62	88	1239.25	1284.443313	3.65%	8.26	8.56
Dy-162	162	66	96	1324.11	1385.331685	4.62%	8.17	8.55
Yb-172	172	70	102	1392.76	1469.133262	5.48%	8.10	8.54
W-183	183	74	109	1465.53	1561.208977	6.53%	8.01	8.53
Pt-194	194	78	116	1539.58	1652.970554	7.37%	7.94	8.52
Au-197	197	79	118	1559.40	1673.675529	7.33%	7.92	8.50
Hg-200	200	80	120	1581.21	1702.923901	7.70%	7.91	8.51
Pb-204	204	82	122	1605.34	1738.948651	8.32%	7.87	8.52

Tl-205	205	81	124	1615.09	1740.84469	7.79%	7.88	8.49
Pb-208	208	82	126	1636.44	1769.027241	8.10%	7.87	8.50

No other theoretical model has been able to achieve such a tight prediction of binding energy (numerical curve-fitting of the semi-empirical formula is not a theoretical model) with only *one* variable. This feature is an unprecedented success for the electromagnetic model in obtaining such results. The numbers for the calculated binding energy are generated from the computer simulation of each nuclide using the electromagnetic equations. (Experimental data is extracted from reference [88].) Current nuclear models using the *residual* chromo dynamic model and the Schrödinger equation have trouble modeling ${}^2\text{H}$ with six quarks. However, using electromagnetic equations, nuclides as large as copernicium ${}^{283}\text{Cn}$ have easily been modeled.

This model has applied the laws of electromagnetics directly to the quarks, and combined this feature together with aspects of the *residual* chromo dynamic model and the cluster model.

This model assumes the laws of electromagnetics are valid inside a nucleus, and that these laws should not be disregarded. This model asserts that is the electromagnetic properties of the quarks within the nucleus that create the nuclear force and hold the nucleons in a nucleus together. The electromagnetic forces and energies cause the nuclides to fall into the lowest energy state and configuration. It is asserted that this electromagnetic energy and the specific lowest energy configurations of the nuclides are features that give the nuclides certain behaviors, such as binding energy, large quadrupole moments, excited states, and particle decay.

Rather than disregarding the electromagnetic forces and energies of the quarks, when taken into full account and understanding, the electromagnetic forces inside a nucleus can explain much about nuclear behavior. A better understanding of the nuclear behaviors can be gained through this model by applying this knowledge and insight. Only the slight decrease in binding energy per nucleon that is seen of the largest nuclides can not be explained by the electromagnetic force.

In conclusion, a significantly large part of the Nuclear Force, that force which binds together the nucleons in a nucleus, has been directly unified to the Electromagnetic Force.

References

- [1] K. N. Mukhin, *Experimental Nuclear Physics, Volume 1, Physics of Atomic Nucleus*. Mir Publishers, Moscow, p. 120, 1987.
- [2] S. Sharma, *Atomic and Nuclear Physics*. Dorling Kindersley Pvt. Ltd., New Delhi, p.286, 2008.
- [3] R. Eisberg, R. Resnick, *Quantum Physics of Atoms, Molecules, Solids, Nuclei, and Particles*, Wiley, New York, pp 509-549, 1985.
- [4] J. Lilley, *Nuclear Physics Principles and Applications*, Wiley, Chichester, p 35, 2001.
- [5] G. Gamow, Quantum theory of the atomic nucleus, *Z. Phys.* 51: 204, 1928.
- [6] C. F. von Weizsäcker, Zur theorie der kernmassen. *Zeitschrift für Physik* (in German), 96 (7–8): 431–458, 1935.
- [7] G. Gamow, *GAMOW'S DESCRIPTION OF THE "LIQUID DROP MODEL" OF THE ATOMIC NUCLEUS In the Proceedings of the Royal Society of London Series A. Vol. CXXIII "DISCUSSION ON STRUCTURE OF ATOMIC NUCLEI" pp 373-390. Gamow's contribution of pp. 386-387.* Royal Society, London, pp.373-390, 1929.
- [8] H. Yukawa, On the interaction of elementary particles, *Proc. Phys. -Math. Soc. Japan*, 17: 48, 1935.
- [9] L. R. Hafstad and E. Teller, The alpha-particle model of the nucleus, *Phys. Rev.* 54: 681, 1938.
- [10] A. H. Wuosmaa, et al., Evidence for Alpha-Particle Chain Configuration in ${}^{24}\text{Mg}$, *Nuclear Physics*, A553: 563c-566c, 1993.
- [11] A. H. Wuosmaa, et al., Evidence for Alpha-Particle Chain Configuration in ${}^{24}\text{Mg}$, *Physical Review Letters*, 68, 9: 1295-1298, 1992.
- [12] B.M. Nyako' et al., *Phys. Rev. Lett.*, 52: 507, 1984.
- [13] S. P. G. Chappell et al., *Phys. Rev. Lett.*, B444: 260, 1998.
- [14] M. D'Agostino, Focus: rod-shaped nucleus, *Phys. Rev. Focus*, 28: 10, 2011.
- [15] H. Horiuchi, K Ikeda, *Progress in Theoretical Physics*, 40: 277, 1968.
- [16] I. Hamamoto, B. Mottelson, Shape deformations in atomic nuclei, *Scholarpedia*, vol. 7(4): 10693, 2012.
- [17] H. Horiuchi, Coexistence of cluster states and mean-field-type states, *J. Phys. G: Nucl. Part. Phys.*, 37: 064021, 2010.
- [18] A. C. Merchant, W. D. M. Rae, Systematics of alpha-chain states in 4 N-nuclei. *Nuclear Physics*, A549: 431-438, 1992.
- [19] N. Itagaki, et al., Exotic cluster structure in light nuclei, *Journal of Physics: Conference Series*, 420: 012080, 2013.
- [20] T. Ichikawa, J. A. Maruhn, N. Itagaki, and S. Ohkubo, Linear chain structure of four- α clusters in ${}^{16}\text{O}$, *Physics Review Letters*, 107: 112501, 2011.
- [21] L. Zamick, D. C. Zheng, Linear α -chain states in nuclei, *Zeitschrift für Physik A Hadrons and Nuclei*, 349, 3-4: 255-257, 1994.
- [22] B. R. Fulton, The Six Alpha Chain state story – from Strasborg to Rab, in *Proceedings of the 7th International Conference on Clustering Aspects of Nuclear Structure and Dynamics*. M. Korolija, Z. Basrak, R. Caplar, Eds. London: World Scientific Publishing Company. Pte. Ltd., p122-129, 2000.

- [23] C. Beck, State of the Art in Nuclear Cluster Physics, *Journal of Physics: Conference Series*, 569: 012002, 2014. doi: 10.1088/1742-6596/569/1/012002.
- [24] K. N. Mukhin, *Experimental Nuclear Physics, Volume 1, Physics of Atomic Nucleus*, Mir Publishers, Moscow, p.133, 1987.
- [25] Ivanenko, D.D., "The neutron hypothesis", *Nature*. 129 (3265): p. 798, 1932.
- [26] M. G. Mayer, *Phys. Rev.*, 75, p. 1969, 1949.
- [27] M. G. Mayer, J. H. D. Jensen, *Elementary Theory of Nuclear Shell Structure* Wiley, New York, 1955.
- [28] Nilsson, S.G. "Binding states of individual nucleons in strongly deformed nuclei," *Kgl. Danske Videnskab. Selskab., Mat.-fys Medd.*, Vol: 29, No. 16, 1955.
- [29] B. A. Brown, B. H. Wildenthal, Status of the nuclear shell model, *Ann. Rev. Nucl. Part. Sci.*, 38: 29-66, 1988.
- [30] A. Bohr, R. B. Mottelson, *Nuclear Structure Vol. I*, W. A. Benjamin Inc., 1969; World Scientific, Singapore, 1998.
- [33] A. Bohr, R. B. Mottelson, *Nuclear Structure, Vol. II* W. A. Benjamin Inc., 1975; World Scientific, Singapore, 1998.
- [32] A. Bohr, Rotational Motion in Nuclei, *Rev. Mod. Phys.* 48(1976), 365.
- [33] B. Mottelson, Elementary modes of excitation in the nucleus, *Rev. Mod. Phys.* 48(1976), 37.
- [34] R. Eisberg, R. Resnick, *Quantum Physics of Atoms, Molecules, Solids, Nuclei, and Particles*, Wiley, New York, pp 545-549, 1985.
- [35] K. S. Krane, *Introductory Nuclear Physics*, Wiley, New York, pp.134-146, 1988.
- [36] J. D. McGervey, *Introduction to Modern Physics*, Academic Press, New York, pp.498-499, 1971.
- [37] H. Georgi, Effective field theory, *Annual Review of Nuclear and Particle Science*, 43: 209-252, 1993.
- [38] R. B. Wiringa, V. G. J. Stoks, and R. Schiavilla, Accurate nucleon–nucleon potential with charge-independence breaking, *Physical Review C*, 51:38, 1995.
- [39] G. Vayenas, S. Souentie *Gravity, Special Relativity and the Strong Force*, Springer, New York, pp 25-27, 2012.
- [40] R Machleidt, Nuclear Forces. *Scholarpedia*, 9(1):30710, 2014.
- [41] Bernard Schaeffer, "Electric and Magnetic Coulomb Potentials in the Deuteron", *Advanced Electromagnetics Journal*, 2: 69-72, 2013.
- [42] Gell-Mann (1964). "A Schematic Model of Baryons and Mesons". *Physics Letters*. 8 (3):214-215. doi: 10.1016/S0031-9163(64)92001-3
- [43] G. Zweig (1964). "An SU(3) Model for Strong Interaction Symmetry and its Breaking" (PDF). CERN-TH-401.
- [44] G. Zweig (1964). "An SU(3) Model for Strong Interaction Symmetry and its Breaking: II". CERN-TH-412.
- [45] M. Gell-Mann (2000) [1964]. "The Eightfold Way: A Theory of Strong Interaction Symmetry". In M. Gell-Mann, Y. Ne'eman (ed.). *The Eightfold Way*. Westview Press. p. 11. ISBN 978-0-7382-0299-0. Original: M. Gell-Mann (1961). "The Eightfold Way: A Theory of Strong Interaction Symmetry". Synchrotron Laboratory Report CTSL-20. California Institute of Technology. doi:10.2172/4008239
- [46] J. Ashman, EMC Collaboration, A measurement of the spin asymmetry and determination of the structure function g_1 in deep inelastic muon-proton scattering, *Physics Letters B*, 206 (2): 364, 1988.
- [47] R. L. Jaffe, Where does the proton really get its spin?, *Physics Today*, Sept 1995: 24 1995.
- [48] S. Brodsky, J. Ellis, M. Karliner, Chiral symmetry and the spin of the proton, *Phys. Lett. B*, 206: 309, 1988.
- [49] X. Zheng, J. P. Chen, Z.-E. Meziani. The Spin Structure of the Nucleon in the Valence Quark Region, *Phys. Rev. C*, 65: 065205, 2002.
- [50] A. V. Belitsky, Xiangdong Ji, Feng Yuan, *Phys. Rev. Lett.*, 91: 092003, 2003.
- [51] A. Thomas, Interplay of Spin and Orbital Angular Momentum in the Proton, *Physical Review Letters*, 101 (10): 102003, 2008.
- [52] C. T. H. Davies, *et al.*, Precise Charm to Strange Mass Ratio and Light Quark Masses from Full Lattice QCD, *Physical Review Letters*, 104 (13): 132003, 2010.
- [53] A. Antognini, *et al.* Proton Structure from the Measurement of 2S-2P Transition Frequencies of Muonic Hydrogen, *Science*, 339 (6118): 417, 2013.
- [54] Sinya Aoki *et al.* (2012). Lattice QCD approach to nuclear physics. arXiv: 1206.5088 [hep-lat]
- [55] D. M. Brink. History of cluster structure in nuclei, *J. Phys.: Conf. Ser.*, 111: 012001, 2008.
- [56] S. A. Afzal, A. A. Z. Ahmad, and S. Ali, Systematic survey of the alpha-alpha interaction, *Rev. Mod. Phys.*, 41(1): 247-273, 1969.
- [57] M. Freer, The clustered nucleus—cluster structures in stable and unstable nuclei, *Reports on Progress in Physics*, 70: 2149, 2007.
- [58] B. R. Fulton, Clustering in nuclei: nuclear chains, nuclear molecules and other exotic states of nuclear matter, *Contemporary Physics*, 40: 299-311, 1999.
- [59] T. Kawabata *et al.*, $2\alpha + t$ cluster structure in ^{11}B , *Phys. Lett.*, B646: 6-11, 2007.
- [60] K. Ikeda, N. Tagikawa and H. Horiuchi, "The Ikeda Diagram". *Prog. Theo. Phys. Suppl.* extra number: p 464, 1968.
- [61] N. L. Bowen, A Simple Calculation of the Inter-Nucleon Up-to-Down Quark Bond and its Implications for Nuclear Binding, *J. Condensed Matter Nucl. Sci.* 29 (2019) 249–259
- [62] D. Halliday, R Resnick, *Fundamentals of Physics*, Wiley, New York, p.477, 1974.

- [63] P. Lorrain, D. Corson, *Electromagnetic Fields and Waves*, Freeman and Company, San Francisco, p72-76, 1970.
- [64] D. Giancoli, *Physics Principles with Applications*, Prentice Hall, Upper Saddle River, New Jersey, pp.509-510, 1998.
- [65] G. E. Owen, *Electromagnetic Theory*, Allen and Bacon, Inc., Boston, pp.21-26, 1963.
- [66] D. Halliday, R Resnick, *Fundamentals of Physics*, Wiley, New York, p.537-571, 1974.
- [67] P. Lorrain, D. Corson, *Electromagnetic Fields and Waves*, Freeman and Company, San Francisco, pp.292-299, 1970.
- [68] D. Giancoli, *Physics Principles with Applications*, Prentice Hall, Upper Saddle River, New Jersey, pp.588-612, 1998.
- [69] G. E. Owen, *Electromagnetic Theory*, Allen and Bacon, Inc., Boston, p.205, 1963.
- [70] K. Yosida, *Theory of Magnetism*, Springer, New York, p.13, 1996.
- [71] D. J. Griffiths, *Introduction to Electrodynamics*, 3rd Edition; Prentice Hall, Upper River Saddle New Jersey, 2007, p 281.
- [72] D. Halliday, R Resnick, *Fundamentals of Physics*, Wiley, New York, p.571, 1974.
- [73] M.E. Peskin, D.V. Schroeder, *An Introduction to Quantum Field Theory*, Perseus Books, Reading Massachusetts, pp.175-198, 1995.
- [74] D.H. Perkins, *Introduction to High Energy Physics*, Addison Wesley, Reading Massachusetts, pp.201-202, 1982.
- [75] P. Lorrain, D. Corson, *Electromagnetic Fields and Waves*, Freeman and Company, San Francisco, pp.64-70, 1970.
- [76] A. J. Buchmann, et al., Intrinsic quadrupole moment of the nucleon, arXiv:hep-ph/0101027, Feb. 2008.
- [77] G. Neyens, Nuclear magnetic and quadrupole moments for nuclear structure research on exotic nuclei, *Reports on Progress in Physics*, 66: 633, 2003.
- [78] N. E. Holden, "Table of the Isotopes", in D.R. Lide, Ed., *CRC Handbook of Chemistry and Physics*, 84th Ed., CRC Press, Boca Raton, FL, 2004.
- [79] S. Raman, C.W.Nestor, P. Tikkanen, "Transition Probability from the Ground to the First 2+ state of Even-Even Nuclides", in B. Pritychenko. Ed., *Atomic Data and Nuclear Data Tables*, vol. 78, Elsevier Inc., Cambridge, MA. pp1-128 (2001).
- [80] K. N. Mukhin, *Experimental Nuclear Physics, Volume 1, Physics of Atomic Nucleus*. Mir Publishers, Moscow, p. 62-68, 1987.
- [81] J. D. McGervey, *Introduction to Modern Physics*, Academic Press, New York, pp.470-475, 1971.
- [82] K. S. Krane, *Introductory Nuclear Physics*, Wiley, New York, pp.49-57, 1988.
- [83] H. De Vries, C. W. De Jager, and C. De Vries, Nuclear charge-density-distribution parameters from elastic electron scattering. *Atomic Data and Nuclear Data Tables*, 36: 495-536, 1987.
- [84] E. Schrödinger, An undulatory theory of the mechanics of atoms and molecules, *Physical Review*, vol. 28 (6), pp. 1049–1070, 1926.
- [85] K. S. Krane, *Introductory Nuclear Physics*, Wiley, New York, p.144, 1988.
- [86] J. D. McGervey, *Introduction to Modern Physics*, Academic Press, New York, p.498, 1971.
- [87] C.A. Bertulani, *Nuclear Physics in a Nutshell*, Princeton University Press, Princeton New Jersey, p.155, 2007.
- [88] National Nuclear Data Center, information extracted from the NuDat 2 database, <http://www.nndc.bnl.gov/nudat2/>